Journal of Power Sources 194 (2009) 1068–1074

Contents lists available at ScienceDirect

Journal of Power Sources

journal homepage: www.elsevier.com/locate/jpowsour

Electrochemical stability of bis(trifluoromethanesulfonyl)imide-based ionic liquids at elevated temperature as a solvent for a titanium oxide bronze electrode

Junyoung Mun, Yoon Seok Jung[1], Taeeun Yim, Hyun Yeong Lee, Hyo-Jin Kim, Young Gyu Kim, Seung M. Oh*

Department of Chemical and Biological Engineering, Research Center for Energy Conversion & Storage, Seoul National University, 56-1, Shillim-dong, Gwanak-ku, Seoul 151-744, Republic of Korea

ARTICLE INFO

Article history:
Received 22 October 2008
Received in revised form 13 April 2009
Accepted 25 May 2009
Available online 9 June 2009

Keywords:
Lithium-ion battery
Room-temperature ionic liquids
Titanium oxide bronze
Thermal stability
Cathodic stability
Electrolyte decomposition

ABSTRACT

Four different electrolytes are prepared by dissolving a Li salt in three different room-temperature ionic liquids (RTILs) and also in a conventional organic solvent. The cathodic (electrochemical reduction) stability of these electrolytes is compared at both ambient and elevated temperature by potential cycling on a TiO_2-B electrode. At room temperature, the stability of pyrrolidinium- and piperidinium-based RTILs is comparable with that of the carbonate-based organic solvent, which is in contrast to the severely decomposed imidazolium-based RTIL. At elevated temperature (120 °C), the imidazolium-based RTIL undergoes even more significant cathodic decomposition that results in the deposition of a resistive surface film and leads to eventual cell degradation. By contrast, the cathodic decomposition and concomitant film deposition are not serious with pyrrolidinium- and piperidinium-based RTILs even at this high-temperature, so that the TiO_2-B/Li cell operates with reasonably good cycle performance. The latter two RTILs appear to be promising solvents for lithium-ion batteries that are durable against occasional exposure to high-temperature.

1. Introduction

During the past decade, lithium-ion batteries (LIBs) have been a major power source for portable electronic devices such as mobile phones and notebook computers. Recently, the issues of oil price and global warming have brought an increasing awareness to the need for more fuel-efficient and less-polluting hybrid electric vehicles (HEVs), for which LIBs are being considered as replacements for the present nickel-metal hydride cells [1–3]. The performance of LIBs, however, still falls short of the requirements for many transportation applications with respect to specific energy, specific power, cell life, and safety characteristics. The safety characteristics of LIBs are often deeply associated with the high-temperature stability of the cell constituents. For instance, thermal runaway is often triggered by internal/external electric shorts or over-charging and is accompanied by decomposition of the electrode/electrolyte constituents and the eventual ignition of combustible ingredients. Thermally stable and non-flammable electrodes/electrolytes may thus reduce the danger of thermal runaway. Cell life is also affected by the thermal stability of electrodes/electrolytes. That is, if these materials are vulnerable to decomposition under occasional high-temperature exposure, the cells deteriorate and fail prematurely [4–6].

Room-temperature ionic liquids (RTILs) have been proposed as solvents for long-lived and safer LIBs, since they are generally non-flammable and have low volatility as well as superior thermal stability [7,8]. Unfortunately, however, the cathodic (electrochemical reduction) stability of RTILs is poorer than that of conventional organic solvents [9–12]. For instance, it has been reported that imidazolium-based RTILs are cathodically decomposed at <1.0 V (*vs.* Li/Li^+) on a glassy carbon electrode at room temperature [10]. By contrast, pyrrolidinium- and piperidinium-based RTILs exhibit better cathodic stability on the same inert electrode and are decomposed at <0.4–0.5 V [11,12]. Up to now, however, there have been few detailed reports of the cathodic stability of these RTILs at elevated temperatures.

The prime aim of this work is to examine whether RTILs can be used as solvents for long-lived LIBs. To this end, the high-temperature electrochemical stability of RTILs and the elevated temperature cell degradation mechanism have been examined. Three different electrolytes are prepared by dissolving a Li salt in three different RTIL solvents based on imidazolium, pyrrolidinium and piperidinium, and their high-temperature (120 °C) cathodic stability is examined by cyclic voltammetry and charge–discharge

* Corresponding author. Tel.: +82 2 880 7074; fax: +82 2 872 5755.
E-mail address: seungoh@snu.ac.kr (S.M. Oh).
[1] Present address: Department of Mechanical Engineering, University of Texas at Austin, Austin, TX 78712, USA.

0378-7753/$ – see front matter © 2009 Elsevier B.V. All rights reserved.
doi:10.1016/j.jpowsour.2009.05.048

cycling. The deposition of a resistive surface film and an impedance increase, which may be the result of electrolyte decomposition, are examined by means of electron microscopy and impedance spectroscopy. The results are further compared with those obtained with a conventional organic solvent (ethylene carbonate + diethyl carbonate). A titanium oxide bronze (TiO_2-B) phase is used as the electrode, since its lithiation/de-lithiation potential lies within the electrochemical stability window of common RTILs at room temperature [13,14].

2. Experimental

2.1. Materials

Three different RTILs, which have the same anion but different cations, were prepared according to methods reported elsewhere [12,15,16]. The prepared RTILs were EMI-TFSI, PMPyr-TFSI and PMPip-TFSI, where EMI is 1-ethyl-3-methylimidazolium, PMPyr is 1-propyl-1-methylpyrrolidinium, PMPip is 1-propyl-1-methylpiperidinium, and TFSI is bis(trifluoromethanesulfonyl)imide. The molecular structures are shown in the inset of Fig. 2. For the preparation of electrolytes, 1.0 M lithium bis(trifluoromethanesulfonyl)imide (Li-TFSI, 3M, battery grade) was dissolved in the above RTILs and also in a mixture of ethylene carbonate (EC) and diethyl carbonate (DEC) (Cheil Industry, Korea) (1:1 vol. ratio).

The electrode material, titanium oxide bronze (TiO_2-B), was prepared by modifying the method of Marchand et al. [17]. In the first step, $K_2Ti_4O_9$ was obtained by heat-treatment of a ball-milled mixture of KNO_3 (Aldrich) and TiO_2-anatase (Aldrich) (1:2 mol. ratio) for 6 h under an argon atmosphere. The resulting $K_2Ti_4O_9$ powder was ball-milled again and hydrolyzed for 3 days in 0.5 M HNO_3 to obtain a $H_2Ti_4O_9$ precipitate. After washing with de-ionized water, the precipitate was filtered and heated at 500 °C for 15 h under air to obtain the TiO_2-B powder. Power X-ray diffraction (XRD) patterns were obtained with a D8-Brucker diffractometer equipped with Cu Kα radiation (1.54056 Å).

2.2. Electrochemical characterizations

For the preparation of TiO_2-B-containing composite electrodes, a slurry of TiO_2-B powder, Super-P (as a carbon additive for conductivity enhancement) and polyvinylidenefluoride (PVdF, as a binder) (70:20:10 wt. ratio) was coated on a copper current-collector and then dried at 120 °C and pressed. Coin-type half-cells were fabricated with the composite electrode, Li foil was used for both the counter and reference electrodes, and a glass filter (Advanter, GA-55, thickness = 0.21 mm and pore size = 0.6 μm) served as a separator.

Galvanostatic discharge–charge cycling was made using a Toscat-2100 cycler. Cyclic voltammograms were obtained with a CHI660A electrochemical workstation and a.c. impedance measurements were made using the same instrument in the frequency range of 5 mHz–100 kHz with an amplitude of 10 mV. In this presentation, lithiation is expressed as discharging and de-lithiation as charging.

2.3. Field-emission scanning electron microscope (FE-SEM) and X-ray photoelectron spectroscopy (XPS) study

For post mortem FE-SEM (Model JSM-6700F, JEOL) and XPS analysis, the cells were dismantled in a glove-box and the electrodes were washed with dimethyl carbonate. A hermetic vessel was used to transfer the samples from the glove-box to the instrument chamber. The XPS data were collected in an ultra-high vacuum multipurpose surface analysis system (Sigma probe, Thermo, UK) that operated at a base pressure of $<10^{-10}$ mbar. The photoelectrons were excited by a Al Kα (1486.6 eV) anode at a constant power of 100 W (15 kV and 10 mA); the X-ray spot size was 400 μm. During data acquisition, a constant-analyzer-energy mode was used at a pass energy of 30 eV and a step of 0.1 eV. The binding energy was calibrated by the C 1s peak at 285 eV that was obtained from hydrocarbon contamination.

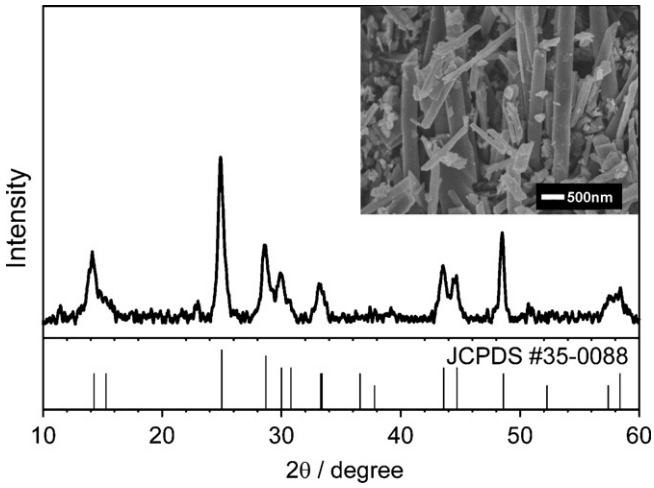

Fig. 1. X-ray diffraction (XRD) pattern of prepared TiO_2-B powder. FE-SEM image provided in inset.

3. Results and discussion

The XRD pattern of the prepared TiO_2-B powder is shown in Fig. 1. The diffraction peaks match well with those for the monoclinic TiO_2-B phase (Joint Committee on Powder Diffraction Standards #35-0088). Any diffraction peaks belonging to the other polymorphs of TiO_2, such as anatase and rutile, are not detected. The FE-SEM image (inset) shows that the TiO_2-B powder has a rod-like morphology [18].

The first discharge–charge voltage profiles of TiO_2-B/Li cells, which were recorded in four different electrolytes at room temperature, are presented in Fig. 2. The cells cycle with reasonable reversibility within the potential range of 1.0–2.0 V (*vs.* Li/Li^+), which is far above that for graphite electrodes [19,20]. The four electrolytes give rise to comparable discharge (lithiation) and charge

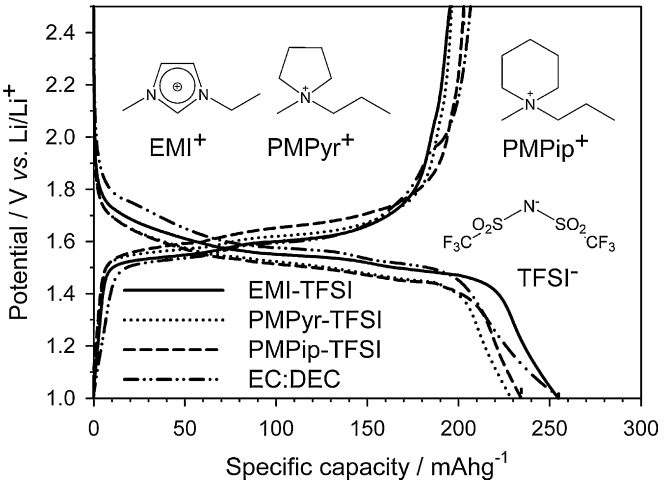

Fig. 2. Galvanostatic discharge–charge voltage profile of TiO_2-B/Li cell obtained in four different electrolytes. Molecular structure of cations and anion provided in inset. Current density = 25 mA g^{-1} and T = 25 °C.

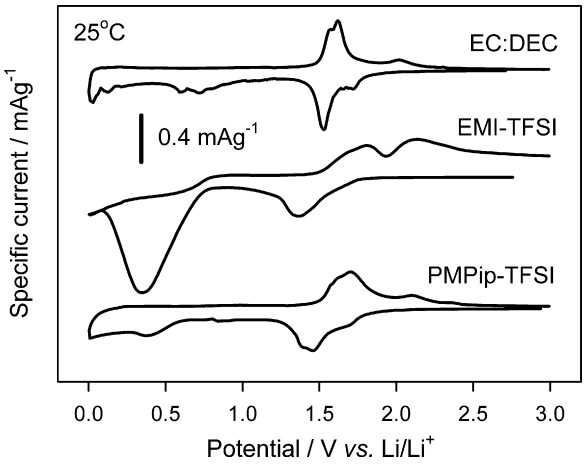

Fig. 3. Cyclic voltammograms for TiO_2-B electrode in three different electrolytes; solvents indicated in inset. Voltammogram for PMPyr-TFSI is largely the same as that for PMPip-TFSI (omitted). Note evolution of large reduction current at 0.4 V with EMI-TFSI. Scan rate = 0.1 mV s^{-1} and T = 25 °C.

(de-lithiation) capacities. The de-lithiation capacity and coulombic efficiency in the first cycle are: EMI-TFSI: 195 mAh g^{-1}, 77%; PMPyr-TFSI: 196 mAh g^{-1}, 86%; PMPip-TFSI: 202 mAh g^{-1}, 87%; and EC:DEC: 196 mAh g^{-1}, 85%, respectively. Note, however, that the discharging and charging electrode overpotential for the organic carbonates is smaller than that observed for the ionic liquids. This must be due to the lower viscosity and higher conductivity of the carbonate-based electrolyte.

In order to examine the cathodic stability of RTILs at <1.0 V, cyclic voltammograms were recorded by extending the negative limit down to 0.0 V (Fig. 3). In the three voltammograms, the cathodic current appears at 1.8–1.3 V and the anodic current at 1.4–2.0 V, which must be associated with lithiation and de-lithiation into/from the TiO_2-B electrode, respectively. A noticeable feature that evolves with the imidazolium-based ionic liquid (EMI-TFSI) is the large reduction current peak at 0.4 V and the oxidation peak at >2.1 V. Such intense redox peaks do not evolve in the carbonate-based (EC + DEC) or the piperidinium-based ionic liquid (PMPip-TFSI) electrolyte. In short, both PMPip- and PMPyr-based RTILs, and the organic carbonates are cathodically stable down to 0.0 V, but the imidazolium-based RTIL is unstable. The poor cathodic stability of EMI-based ionic liquids has been ascribed to the presence of an acidic proton located at the 2-C position [21,22]. The poor cathodic stability of EMI-TFSI is reflected as a poor cycleability, as shown in Fig. 4, in which the lower cut-off voltage is varied while the upper limit is fixed at 2.5 V. When the TiO_2-B/Li cell is cycled at 1.2–2.5 V, in the potential range that electrochemical reduction (electrolyte decomposition) of EMI-TFSI is not severe (Fig. 3), the working cell in EMI-TFSI gives comparable cycle performance to that observed with the other solvents. On the other hand, when the lower cut-off is extended down to 0.6 V, where the electrochemical reduction of EMI-TFSI is significant, the working cell with EMI-TFSI shows rapid capacity fading. By contrast, the cells cycled in the other solvents, which are cathodically stable down to 0.0 V (Fig. 3), give reasonable cycle performances even with this low cut-off limit. It will be shown in a later section that the capacity fading is associated with the formation of a resistive surface film that is deposited as a result of electrolyte decomposition.

The high-temperature electrochemical stability of RTILs, which is the main subject in this work, was examined by recording cyclic voltammograms at 120 °C (Fig. 5). A comparison of the data shown in Figs. 3 and 5 reveals that several features become apparent with an increase in the working temperature. First of all, the broad current peaks observed at 1.3–2.0 V at 25 °C (Fig. 3), which are associated with lithiation/de-lithiation, are now resolved into at least three discernable pairs of redox peaks, which must be the result of an increase in the lithiation/de-lithiation rate with increase in temperature. Second, a reduction peak develops at 1.1 V and an oxidation peak at >2.5 V in the votammogram recorded in EMI-TFSI, which are absent in both PMPip-TFSI and PMPyr-TFSI (not shown). This redox peak must correspond to those that appear at 0.4 V and >2.1 V at 25 °C, respectively. The shift of the reduction peak from 0.4 (25 °C) to 1.1 V (120 °C) seems to be due to facilitation of the electrochemical reduction reaction at elevated temperatures. Here, it is noted that the lower stability of the EMI-based ionic liquid at 120 °C when compared with the PMPyr- and PMPip-based RTILs appears to be caused by its lower electrochemical

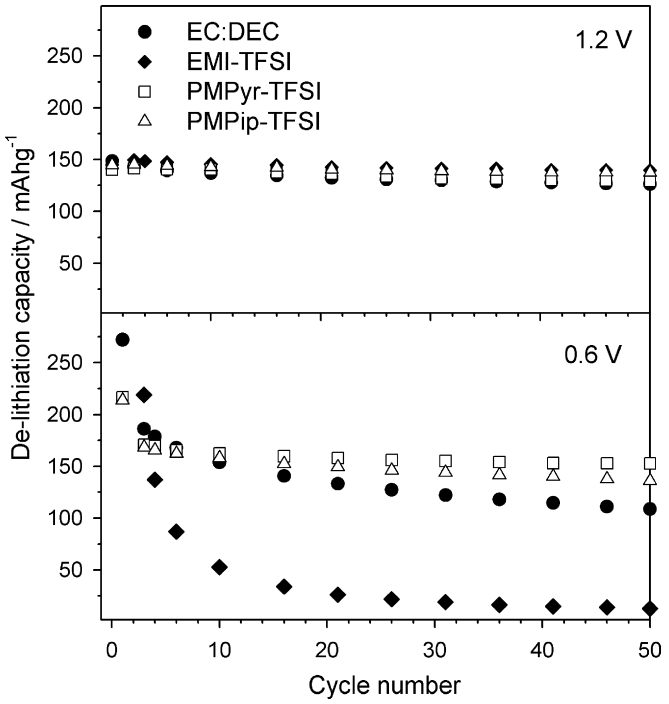

Fig. 4. Cycle performance of TiO_2-B/Li cell obtained with two different lower cut-off potentials at 25 °C. Note cell operated in EMI-TFSI-containing electrolyte degrades rapidly when lower cut-off potential is extended down to 0.6 V. Upper cut-off potential = 2.5 V and current density = 70 mA g^{-1}.

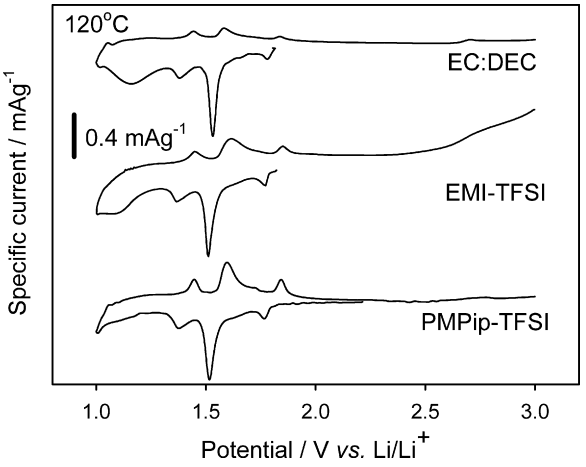

Fig. 5. Cyclic voltammograms for TiO_2-B electrode in three different electrolytes. Voltammogram for PMPyr-TFSI solvent is largely same as that for PMPip-TFSI (omitted). Potential sweep starts toward the negative direction. Note evolution of large reduction current at 1.1 V with the carbonate-based (EC:DEC) and EMI-TFSI solvent. Scan rate = 0.1 mV s^{-1} and T = 120 °C.

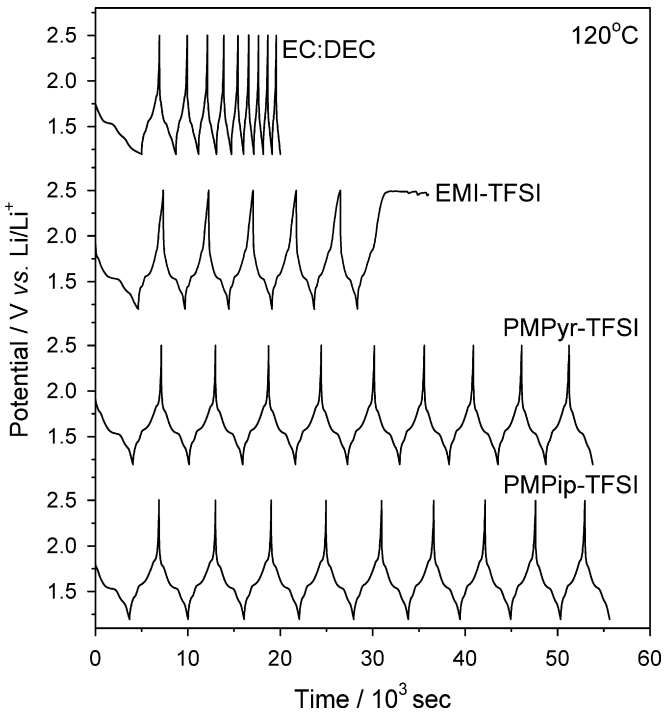

Fig. 6. Galvanostatic discharge–charge voltage profiles obtained with four different electrolytes at 120 °C. Note rapid capacity fading with EC:DEC and cell failure with EMI-TFSI after six cycles. Also note acceptable cycle performance with PMPyr-TFSI and PMPip-TFSI. Cycling was undertaken over in the potential range 1.2–2.5 V at current density of 250 mA g^{-1}.

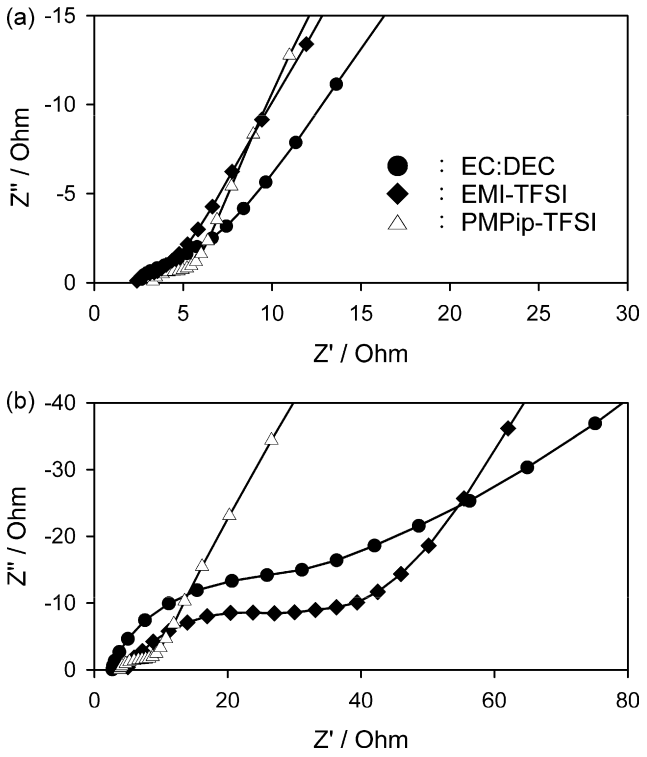

Fig. 7. a.c. impedance spectra for TiO_2-B/Li cell: (a) before cycling and (b) after 5 cycles at 120 °C. Measurements made at discharged state (1.2 V for TiO_2-B electrode). Discharge–charge cycling condition same as for Fig. 6. Note enlargement of semicircles with carbonate-based (EC:DEC) and EMI-TFSI solvent, indicating that a resistive surface film is deposited as a result of electrolyte decomposition.

stability rather than its thermal stability. A separate thermogravimetric analysis (TGA) illustrates that the thermal decomposition temperatures of EMI-TFSI, PMPyr-TFSI and PMPip-TFSI are 430, 417 and 385 °C, respectively [12,23]. The carbonate solvent (EC:DEC), which is cathodically stable down to 0.0 V at 25 °C, decomposes at 120 °C as evidenced by the broad reduction current beginning from 1.3 V. Finally, even if the three pairs of redox peaks that are associated with lithiation/de-lithiation of the TiO_2-B electrode are present at 1.4–1.8 V, the oxidation (de-lithiation from TiO_2-B electrode) peaks are much smaller than the reduction peaks in EC:DEC and EMI-TFSI. Given that electrochemical decomposition is significant in these solvents, it is very likely that the de-lithiation reaction is hindered by the presence of a surface film that is deposited on the TiO_2-B electrode as a result of electrolyte decomposition at 1.3–1.0 V. Note that the de-lithiation current is quite intense in PMPip-TFSI, which is not decomposed at <1.3 V in the negative potential sweep (Fig. 5).

The poor high-temperature electrochemical stability of EC:DEC and EMI-TFSI is clearly manifested as poor cycleability of the TiO_2-B/Li cell, as shown in Fig. 6. The galvanostatic discharge–charge voltage profiles illustrate that the cell is gradually degraded in a ED:DEC solvent, but abruptly fails in EMI-TFSI due to a leakage current that appears at the positive end, which appears to be related to the oxidation reaction occurring at >2.5 V (Fig. 5). The cells operated in PMPyr-TFSI and PMPip-TFSI, however, operate well with excellent cycle performance even at this high-temperature.

The a.c. impedance data shown in Fig. 7 can explain why the cells cycled in EC:DEC and EMI-TFSI show such poor cycle performance. As seen in Fig. 7a, the Nyquist plots obtained before cycling are similar, regardless of the solvents used. The size of each semicircle, which is likely associated with Li^+ ion migration through the surface film and charge-transfer resistance, is comparable, and the Warburg impedance, which is related to mass transfer, appears in the lower frequency region [24]. Detailed analysis was not made in this work. By contrast, the impedance spectra taken after five cycles (Fig. 7b) show a large difference between the solvents used. The cells cycled in PMPip-TFSI and PMPyr-TFSI (not shown) display a marginal increase in the size of the semicircle, whereas a noticeable increase is observed with EC:DEC and EMI-TFSI. From this, the poor cycle performance observed with the latter two solvents can be attributed to an increase in the internal resistance that is the sum of the charge-transfer resistance (R_{ct}) and the film resistance (R_{film}). That is, an increase in R_{film} is readily expected since a thick surface film is deposited on these electrodes. Also, an increment in R_{ct} can be assumed, since the reaction sites for lithiation/de-lithiation into/from the TiO_2-B electrode may be blocked by film deposition [25].

The FE-SEM images taken of the TiO_2-B electrode surface address the reason for the increase in resistance. The electrode cycled in EC:DEC at 25 °C (Fig. 8b) has largely the same surface morphology as that of the pristine electrode (Fig. 8a), in that film deposition is not observed. The electrodes cycled at 120 °C in PMPyr-TFSI (Fig. 8e) and PMPip-TFSI (Fig. 8f) also experience negligible film deposition. Deposition of a thick surface film, however, is apparent on electrodes cycled in EC:DEC (Fig. 8c) and EMI-TFSI (Fig. 8d) at 120 °C. The resistance increase observed with the latter two solvents (Fig. 6) can thus be ascribed to the formation of a resistive surface film (R_{film}) and a concomitant increase in R_{ct}. The diminished de-lithiation current observed in EC:DEC and EMI-TFSI solvents (Fig. 5) can also be explained by an increase in internal resistance due to thick film deposition.

A post mortem XPS analysis was performed to analyze the chemical composition of the surface film, in order to determine the electrochemically decomposed material. Fig. 9 indicates the XPS spectra for Ti 2p, F 1s, C 1s and N 1s photoelectrons, which are obtained with the initial (before cycling) TiO_2-B electrode (c) and those cycled at 120 °C in EC:DEC (a) and EMI-TFSI (b) solvent. The Ti

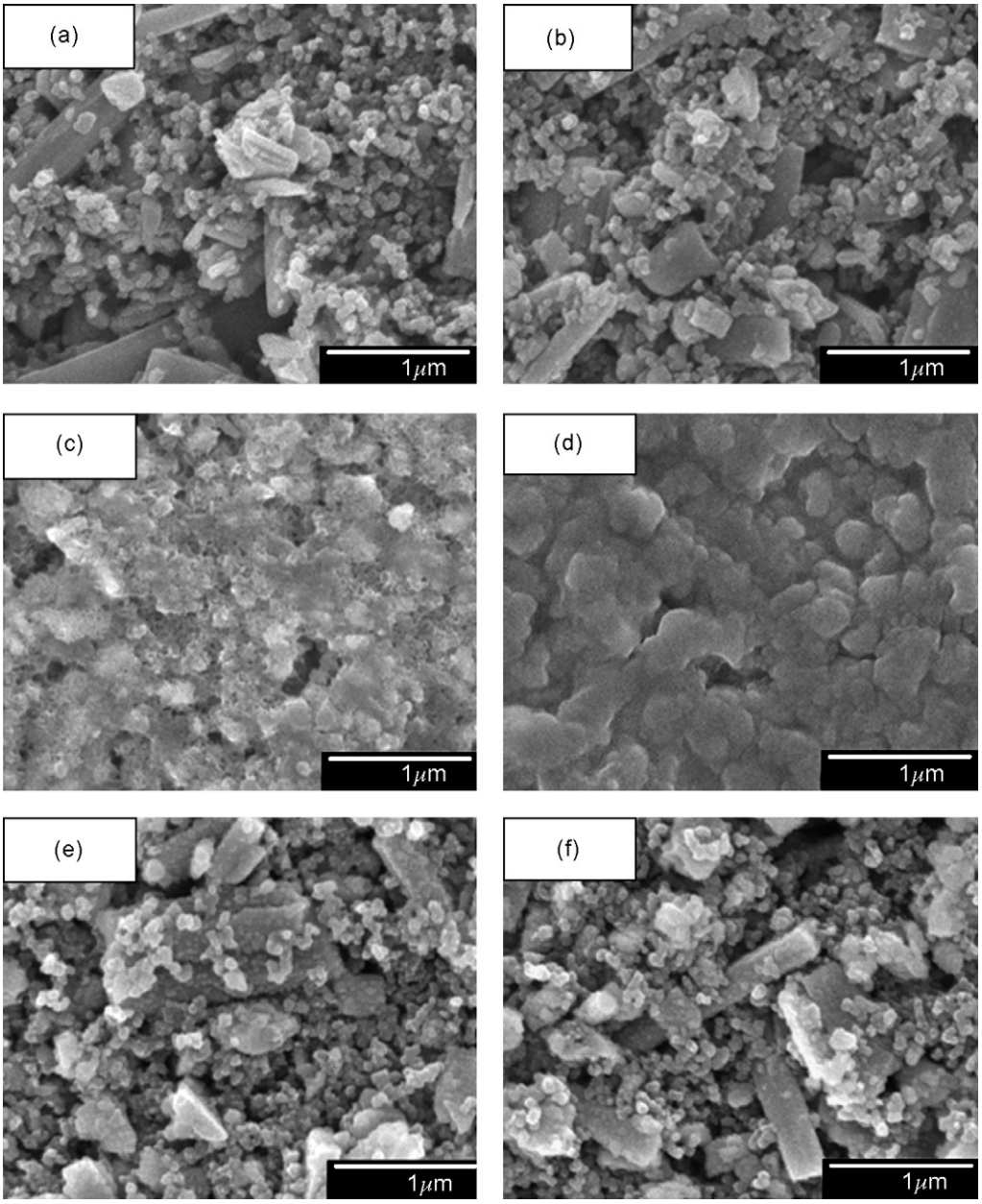

Fig. 8. FE-SEM images of TiO_2-B composite electrode surface: (a) initial state, (b) after 20 cycles at 25 °C in 1.0 M LiTFSI/EC:DEC, (c) after 20 cycles at 120 °C in 1.0 M Li-TFSI/EC:DEC, (d) after 5 cycles at 120 °C in 1.0 M Li-TFSI/EMI-TFSI, (e) after 20 cycles at 120 °C in 1.0 M Li-TFSI/PMPyr-TFSI, and (f) after 20 cycles at 120 °C in 1.0 M Li-TFSI/PMPip-TFSI. Cycling conditions same as for Fig. 6.

$2p_{3/2}$ (459 eV) and Ti $2p_{1/2}$ (464.5 eV) photoelectrons that are emitted from the pristine TiO_2-B electrode are quite abundant, whereas those from the cycled electrodes in EC:DEC (a) and EMI-TFSI solvent (b) are negligible [26]. Considering that photoelectrons are emitted only from the uppermost surface region, it is clear that the surface of the cycled electrodes is covered by a surface film. The F 1s spectra deconvolute to three peaks: LiF at 685.5 eV, CF_2 at 687.5 eV and CF_3 at 689 eV [27,28]. The intense peak at 687.5 eV observed with the initial electrode must be come from the PVdF binder since this fluorinated polymer is placed on the film-free TiO_2-B electrode surface. Emission of the other F 1s photoelectrons (LiF at 685.5 eV and CF_3 at 689 eV) from the film-deposited electrodes strongly suggests that the TFSI anion is decomposed under cathodic polarization. Note that the only way for these fluorinated species to be generated is from the decomposition of the TFSI anion, since the other electrolyte components (cations in ionic liquids and organic carbonates) do not contain any fluorinated functional groups. The C 1s spectra clearly show that the organic carbonates are also decomposed. The C 1s spectra deconvolute to five peaks: graphitic carbons at 284 eV, C–C/C–H at 285 eV, C–N/C–OH at 286 eV, ester at 287 eV, CO_3^{2-}/CF_2 at 290.0–290.5 eV, and CF_3 at 293 eV [27–29]. The most revealing feature is that the C 1s photoelectrons emitted from the CO_3^{2-}/CF_2 groups at 290.0–290.5 eV are much more abundant for the EC:DEC solvent than for the EMI-based ionic liquid. Given that the photoelectrons from the CF_2 moiety that may come from PVdF binder can be neglected due to thick film deposition on these electrodes, the peak at 290.0–290.5 eV is mainly associated with CO_3^{2-} groups that are derived from the organic carbonates (EC:DEC). Also note that an intense peak at 284 eV is observed with the initial TiO_2-B electrode, which must come from the carbon additive (Super-P). The N 1s spectra are resolved into three peaks: quaternary ammonium ions at 402.0 eV, imine at 399.0 eV, and Li_3N at 397.5 eV [30,31].

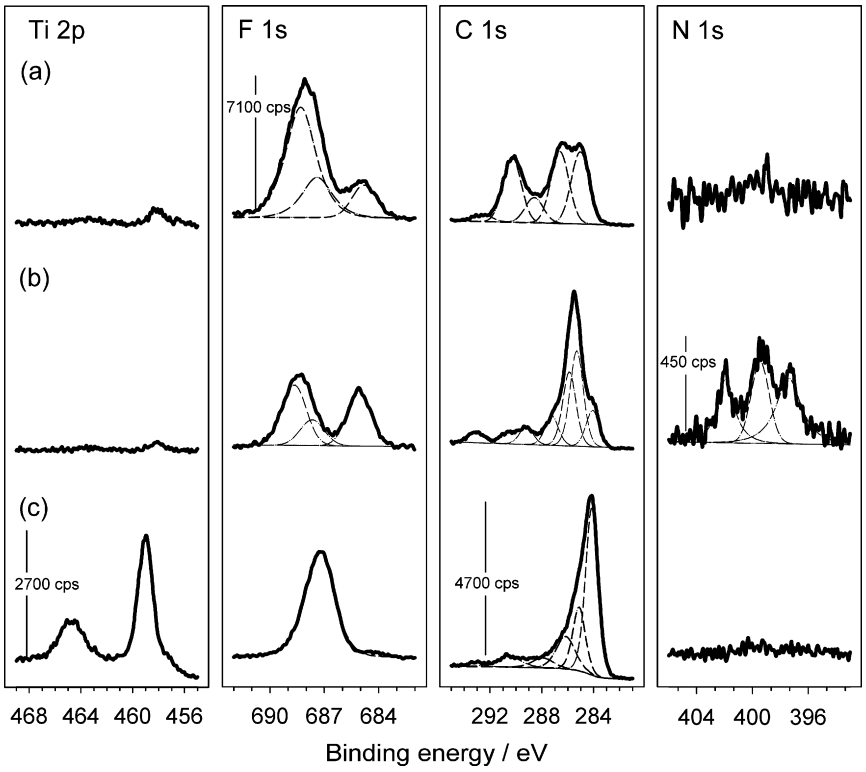

Fig. 9. XPS spectra for Ti 2p, F 1s, C 1s, and N 1s photoelectrons obtained with TiO_2-B electrodes after 5 cycles at 120 °C: (a) EC:DEC, (b) EMI-TFSI, and (c) before cycling.

As seen, two film-deposited electrodes contain the N-species that must come from either the TFSI anion or the EMI cation. The N-containing species on the electrode cycled in EC:DEC should derive from the TFSI anion, whereas those on the electrode cycled in EMI-TFSI both from the TFSI anion or the EMI cation. The big difference in the N 1s peak intensity between two film-deposited electrodes strongly suggests that the EMI cation is also decomposed under cathodic polarization. The electrodes cycled in PMPip-TFSI and PMPyr-TFSI solvent also emit an appreciable number of N 1s photoelectrons (not shown), but their intensity is much smaller than those from the other electrodes. The amount of N 1s photoelectrons emitted from these electrodes is only marginal like that observed with the pristine TiO_2-B electrode. This observation further confirms the electrochemical instability of the TFSI anion at elevated temperature, and the stability of the PMPip and PMPyr cations.

The results presented so far strongly indicate that the high-temperature cycle performance of TiO_2-B/Li cells is greatly affected by the electrochemical stability of the electrolyte used. To confirm this feature further, a control experiment in which the cells were cycled at 25 °C in advance, exposed at 120 °C, and then cycled again at 25 °C was performed. The de-lithiation capacity delivered before and after the high-temperature exposure was compared. During the high-temperature exposure, one group of cells was cycled (1.2–2.5 V) once whereas the other group was stored for 1 day in the charged state (at 2.5 V). Appreciable electrolyte decomposition and film deposition is expected in the former group since the TiO_2-B electrode experiences a cathodic polarization down to 1.2 V during the high-temperature exposure, whereas this undesired feature is likely negligible in the latter group since the TiO_2-B electrode remains in its charged state (at 2.5 V). Fig. 10b illustrates that capacity loss is not significant in the latter group and there by indicates that electrolyte decomposition and film deposition are not severe upon simple (without potential imposition) exposure to high-temperature. The cells that are exposed to a high-temperature with cathodic polarization (down to 1.2 V) show different behaviour, namely, an appreciable capacity loss with the carbonates and EMI-TFSI, but an insignificant loss with PMPyr-TFSI and PMPip-TFSI (Fig. 10a). This feature must be due to a difference in the electrochemical (cathodic) stability of the solvents used. Finally, the largest capacity loss observed with the carbonates among the latter series (Fig. 10b) indicates that the thermal stability of con-

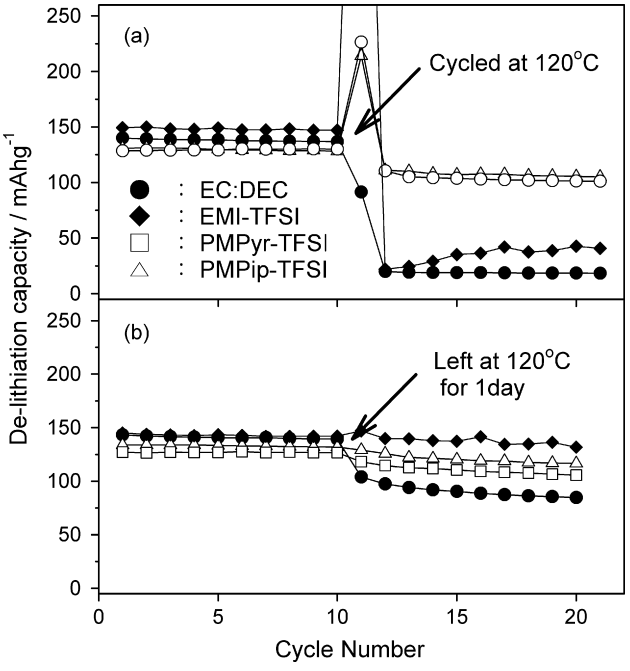

Fig. 10. Capacity loss at high-temperature (120 °C) exposure. De-lithiation capacity monitored with following cycling scheme: initial 10 cycles at 25 °C, exposure at 120 °C, and 10 cycles again at 25 °C. During high-temperature exposure, cells cycled once (a) or left in charged state (2.5 V) for 1 day (b). Note the abnormally high de-lithiation capacity observed with EMI-TFSI during high-temperature exposure, which is caused by leakage current. Cycling was made in potential range of 1.2–2.5 V with a current density of 70 (25 °C) and 250 mA g^{-1} (120 °C).

ventional carbonate solvents is less than that for RTILs, as generally accepted.

4. Conclusions

The cathodic (electrochemical reduction) stability is compared for three different RTILs at both room and elevated temperature, and then further compared with that for a conventional carbonate-based solvent. The cycle performance of the TiO_2-B/Li cell is examined in four different electrolytes and the results are correlated with the cathodic stability of the electrolytes used. The following observations are made:

(i) The EMI-based ionic liquid exhibits the poorest cathodic stability at both room and elevated temperature, and thus has the poorest cycle performance. The carbonate-based electrolyte shows good stability under negative polarization at room temperature, but decomposes at 120 °C. The PMPyr- and PMPip-based ionic liquids are electrochemically stable even at elevated temperature (120 °C), such that the TiO_2-B/Li cell delivers an acceptable cycle performance.
(ii) Electron microscopy images and a.c. impedance data illustrate that resistive film deposition is significant on TiO_2-B electrodes cycled in the cathodically unstable electrolytes. As a result of film deposition, the cells are degraded with impedance increase.
(iii) X-ray photoelectron spectroscopy data illustrate that EMI, TFSI and organic carbonates are cathodically decomposed at 120 °C.

Acknowledgements

The study was supported by the WCU program through KOSEF funded by the Ministry of Education, Science and Technology (400-2008-0230). The authors also wish to acknowledge the Research Center for Energy Conversion and Storage for financial support.

References

[1] M. Winter, J. Besenhard, M. Spahr, P. Novak, Adv. Mater. 10 (1998) 725–763.
[2] O. Bitsche, G. Gutmann, J. Power Sources 127 (2004) 8–15.
[3] K. Lee, Y. Jung, J. Kwon, J. Kim, S. Oh, Chem. Mater. 20 (2008) 447–453.
[4] R. Leising, M. Palazzo, E. Takeuchi, K. Takeuchi, J. Electrochem. Soc. 148 (2001) A838–A844.
[5] J. Jiang, J. Dahn, Electrochim. Acta 49 (2004) 4599–4604.
[6] I. Watanabe, J. Yamaki, J. Power Sources 153 (2006) 402–404.
[7] H. Zheng, H. Zhang, Y. Fu, T. Abe, Z. Ogumi, J. Phys. Chem. B 109 (2005) 13676–13684.
[8] M. Egashira, M. Tanaka-Nakagawa, I. Watanabe, S. Okada, J. Yamaki, J. Power Sources 160 (2006) 1387–1390.
[9] M. Holzapfel, C. Jost, A. Prodi-Schwab, F. Krumeich, A. Wursig, H. Buqa, P. Novak, Carbon 43 (2005) 1488–1498.
[10] M. Galinski, A. Lewandowski, I. Stepniak, Electrochim. Acta 51 (2006) 5567–5580.
[11] V. Baranchugov, E. Markevich, E. Pollak, G. Salitra, D. Aurbach, Electrochem. Commun. 9 (2007) 796–800.
[12] T. Yim, H. Lee, H. Kim, J. Mun, S. Kim, S. Oh, Y. Kim, Bull. Kor. Chem. Soc. 28 (2007) 1567–1572.
[13] M. Zukalova, M. Kalbac, L. Kavan, I. Exnar, M. Graetzel, Chem. Mater. 17 (2005) 1248–1255.
[14] G. Armstrong, A. Armstrong, P. Bruce, P. Reale, B. Scrosati, Adv. Mater. 18 (2006) 2597–2600.
[15] P. Bonhôte, A. Dias, M. Armand, N. Papageorgiou, K. Kalyanasundaram, M. Gratzel, Inorg. Chem. 35 (1996) 1168–1178.
[16] G. Min, T. Yim, H. Lee, D. Huh, E. Lee, J. Mun, S. Oh, Y. Kim, Bull. Kor. Chem. Soc. 27 (2006) 847–852.
[17] R. Marchand, L. Brohan, M. Tournoux, Mater. Res. Bull. 15 (1980) 1129–1133.
[18] T. Brousse, R. Marchand, P. Taberna, P. Simon, J. Power Sources 158 (2006) 571–577.
[19] M. Holzapfel, C. Jost, P. Novak, Chem. Commun. (2004) 2098–2099.
[20] A. Armstrong, G. Armstrong, J. Canales, R. Garcia, P. Bruce, Adv. Mater. 17 (2005) 862–865.
[21] L. Xiao, K. Johnson, J. Electrochem. Soc. 150 (2003) E307–E311.
[22] C. Marisa, C. Buzzeo, Chem. Phys. Chem. 5 (2004) 1106–1120.
[23] H. Ngo, K. Lecompte, L. Hargens, A. McEwen, Thermochim. Acta 357–358 (2000) 97–102.
[24] T. Nam, E. Shim, J. Kim, H. Kim, S. Moon, J. Electrochem. Soc. 154 (2007) A957–A963.
[25] S. Zhang, P. Shi, Electrochim. Acta 49 (2004) 1475–1482.
[26] Z. Liu, L. Hong, B. Guo, J. Power Sources 143 (2005) 231–235.
[27] P. Howlett, N. Brack, A. Hollenkamp, M. Forsyth, D. MacFarlane, J. Electrochem. Soc. 153 (2006) A595–A606.
[28] R. Dedryvere, H. Martinez, S. Leroy, D. Lemordant, F. Bonhomme, P. Biensan, D. Gonbeau, J. Power Sources 174 (2007) 462–468.
[29] D. Ensling, M. Stjerndahl, A. Nyten, T. Gustafsson, J. Thomas, J. Mater. Chem. 19 (2009) 82–88.
[30] R. Jansen, H. Bekkum, Carbon 33 (1995) 1021–1027.
[31] S. Caporali, U. Bardi, A. Lavacchi, J. Electron. Spectrosc. 151 (2006) 4–8.